Int. J. Heat Mass Transfer. Vol. 11, pp. 539–549. Pergamon Press 1968. Printed in Great Britain

THERMAL AND MATERIAL TRANSFER FROM SPHERES
PREDICTION OF LOCAL TRANSPORT

T. R. GALLOWAY and B. H. SAGE
Chemical Engineering Laboratory, California Institute of Technology, Pasadena, California, U.S.A.

(*Received* 14 *July* 1967)

Abstract—From a review of the available experimental data upon local thermal and material transport from spheres, expressions were developed to permit the prediction of such transport as a function of Reynolds number, intensity of turbulence, and polar angle. It was found that the effect of Reynolds number was more pronounced in the separated flow found in the aft hemisphere than in the boundary flows of the forward hemisphere. On the other hand, the intensity of turbulence exerted a much more profound effect on the local transport in the forward hemisphere than in the aft hemisphere. The results are presented in terms of the Frössling number.

NOMENCLATURE

A,	area [ft^2];
A, B, C, D,	coefficients;
b,	specific gas constant [lb/in^2 ft^3/lb °R];
C_p	isobaric heat capacity [Btu/lb °F];
D_C,	Chapman–Cowling diffusion coefficient [ft^2/s];
D_M,	Maxwell diffusion coefficient [lb/s];
d,	diameter [in or ft];
Fs,	Frössling number, $(Nu - 2)/Re^{\frac{1}{2}} Pr_m^{\frac{1}{3}}$ or $(Sh - 2)/Re^{\frac{1}{2}} Sc_m^{\frac{1}{3}}$;
f,	fugacity [lb/ft^2];
h,	heat-transfer coefficient [Btu/s ft^2°F];
k,	mass-transfer coefficient [ft/s];
k,	thermal conductivity [Btu/s ft °F];
$\dot{m}$,	evaporation rate [lb/s ft^2];
N_c,	number of constants;
N_p,	number of data points;
Nu,	local Nusselt number, hd/k;
Nu^*,	macroscopic Nusselt number, $\dot{Q}d/Ak(t_i - t_\infty)$;
$\underset{\bullet}{n}$,	mole fraction;
P,	pressure [lb/in^2 abs. or lb/ft^2 abs.];
Pr,	Prandtl number, κ/ν;
$\dot{Q}$,	total thermal flux [Btu/s];
Re,	Reynolds number, dU/ν;
Sc,	Schmidt number, $\nu/D_{Ck_j} = P\nu/D_{Mk}$;
Sh,	Sherwood number, $kd/D_{Ck_j}, = \dot{m}_k b_k T/D_{Mk} Z(f_k^0/P) \ln(\underset{\bullet}{n}_{j,i}/\underset{\bullet}{n}_{j,\infty})$;
s,	average deviation, fraction (defined in Table 2);
T,	absolute temperature [°R];
t,	temperature [°F];
U_∞,	free-stream velocity [ft/s];
u,	local velocity [ft/s];
$\bar{u}'_{z,f}$,	time average longitudinal fluctuating velocity [ft/s];
w,	weighting factor, $1/(100\,\sigma)$;
Z,	compressibility factor.

Greek symbols

α_t,	apparent level of turbulence, fraction, $[(\bar{u}'_{z,f})^2]^{\frac{1}{2}}/U_\infty$;
κ,	thermometric conductivity [ft^2/s];
ν,	kinematic viscosity [ft^2/s];
σ,	specific weight [lb/ft^3];
σ,	standard deviation, fraction, (defined in Table 2);
ψ,	angle from stagnation [degrees].

Subscripts

c,	calculated;
e,	experimental;
i,	evaluated for interface conditions;
j,	component j;
k,	component k;
m,	molecular property;
∞,	evaluated for free-stream conditions.

Superscripts

m, n,	exponents;
$*$,	macroscopic;
0,	pure component.

INTRODUCTION

A KNOWLEDGE of the local transport from spheres and cylinders significantly enhances the understanding of flow and transport dynamics associated with blunt bodies. One of the earliest analyses of local transport from spheres was the work of Frössling [1]. In addition to a rather complete theoretical analysis, as well as some experimental work involving macroscopic transport to an air stream from drops of different hydrocarbons, the local transport from a naphthalene sphere subliming into an air stream by forced convection was measured. Frössling verified experimentally the predicted Sherwood number at stagnation. Frössling's data for Reynolds numbers up to 100 show the locus of separation and the strong effect of Reynolds number upon transport in the wake.

Garner *et al.* [2–4] carried out measurements of local transport, using solid spheres of benzoic and adipic acids in a water tunnel. In addition to local material transport, Garner studied the effect of Reynolds number on the locus of separation from the aft stagnation point to a position 104° from the forward stagnation at a Reynolds number of 500. The magnitude of the Sherwood numbers reported by Garner appears to be about 40 per cent higher than many other values, such behavior possibly being attributed to elevated free-stream turbulence in Garner's water tunnel. Linton and Sutherland [5] extended local material transport studies in a water tunnel up to a Reynolds number of 7580, and found good agreement with the earlier work of Frössling [1]. Linton [5] also indicated the possibility of effects of free-stream turbulence on material transport.

Effects of free-stream turbulence intensity on the local thermal transport were first systematically investigated with cylinders by Giedt [6] and later by Seban [7], revealing a modest increase in thermal transfer in the forward area with small increases in free-stream turbulence. Such measurements were extended to spheres by Wadsworth [8]. The latter measurements indicated the complicated behavior in the wake, and the displacement of the region of separation with increases in free-stream turbulence. However, no increase in the thermal transfer near stagnation was found with increase in free-stream turbulence since the scale of turbulence was much smaller than the diameter of the sphere. Other investigators [9–12] have measured local transport employing spheres, and of these the work of Xenakis *et al.* [10] is worthy of note. His work involved measurements well into the supercritical region at Reynolds numbers as high as $1{\cdot}6 \times 10^6$. The effect of free-stream turbulence was neglected in the measurements of Xenakis.

Local thermal transfer from spheres with artificially increased free-stream turbulence was studied by Venezian *et al.* [13], using a silver sphere 1·0 in. in diameter. The experimental measurements were made in a rectangular air jet 3 by 12 in. The local heat-transfer coefficient was established from the measured interfacial temperature gradient in the boundary flow normal to the surface. By use of a perforated plate, the free-stream longitudinal turbulence was varied from 0·05 to 0·15. The longitudinal turbulence without a perforated plate was 0·013. Similar studies were reported by Short *et al.* [14] and Brown and Sage [15] for a 0·5-in sphere. Recently, Brown *et al.* [16] measured the local heat-transfer coefficients from a 1·5-in sphere in a water tunnel. They varied the Prandtl number from 2·2 to 6·8 for Reynolds numbers varying from 500 to 480000. Their results demonstrated the marked effect of Reynolds number upon transport in the wake region, as well as the influence of variable properties of the fluid in the boundary flow.

Earlier theoretical work was initiated by Langmuir [17], using the data of Morse [18]. Langmuir showed that the limiting value of what is now known as the Sherwood number was two at zero Reynolds number with no turbulence. Such results confirmed the early experiments of Morse [18], while Fuchs [19] and Frössling [20] predicted the effects of forced convection near stagnation. Several more attempts to obtain an analytical solution have been made and were reviewed by Korobkin [21] and others [22, 23].

A quantitative description of the flow aft of separation has not been realized. Qualitative aspects of such flow have been described by Torobin and Gauvin [24], and Lee and Barrow [25]. Richardson [26, 27] sought to describe empirically separated flows as characterized by the Reynolds number to the two-thirds power. In this paper, some aspects of the influence of free-stream turbulence on local thermal and material transport from spheres will be described.

DISCUSSION

The Nusselt and Sherwood numbers at stagnation were predicted theoretically and verified experimentally [17–20], and may be described by the following expressions for thermal and material transfer:

$$Nu = 2 + 1{\cdot}31\, Re^{\frac{1}{2}}\, Pr_m^{\frac{1}{3}} \tag{1}$$

$$Sh = 2 + 1{\cdot}31\, Re^{\frac{1}{2}}\, Sc_m^{\frac{1}{3}}. \tag{2}$$

Theoretical studies indicate that the coefficient of the Reynolds number should vary with angle from stagnation.

A dimensionless group called the "Frössling number" [28] may be defined by equations (1) and (2) which indicate the variations of the local transport from that at stagnation. In the case of thermal transfer, it assumes the form:

$$Fs = \frac{Nu - 2}{Re^{\frac{1}{2}}\, Pr_m^{\frac{1}{3}}}. \tag{3}$$

Correspondingly, for material transfer:

$$Fs = \frac{Sh - 2}{Re^{\frac{1}{2}}\, Sc_m^{\frac{1}{3}}}. \tag{4}$$

The measured variation of the Frössling number with polar angle by several investigators [8, 10, 13–15] is shown in Fig. 1 for longitudinal levels of turbulence below 0·05. A more complicated behavior in the wake at Reynolds numbers above 2×10^5 is characteristic of nearly all measurements. Transition to supercritical flow alters the flow in the wake, as is indicated qualitatively in Fig. 1.

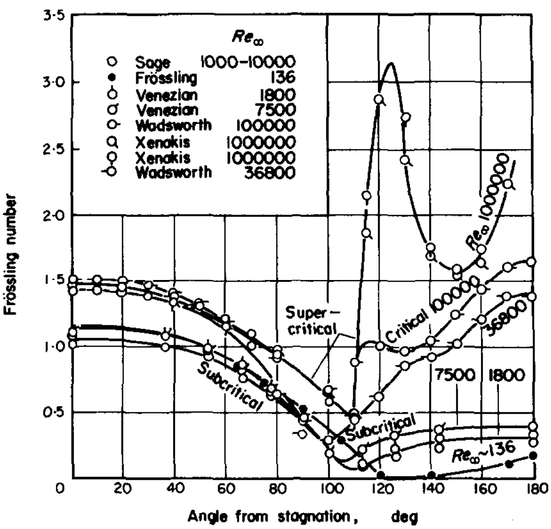

FIG. 1. Effect of polar angle upon local Frössling number.

The available experimental data for local transfer [13–15] corrected for radiant transport were subjected to an integral restraint applied graphically to insure consistency with the measured macroscopic transport. The macroscopic measurements involving the direct determination of the total transport under the same

Table 1. Summary of experimental

Description of sphere material	diameter§	Number of points	Turbulence level min.	Turbulence level max.	Prandtl number min.	Prandtl number max.	Schmidt number min.	Schmidt number max.
porous ceramic	0·5	99	0·013	0·15	—	—	1·2	
silver	0·5	99	0·013	0·15	0·7		—	—
silver	1·0	132	0·013	0·15	0·7		—	—
naphthalene	0·02	66	—	—	—	—	0·6	2·8
benzoic acid	0·38	11	low		—	—	1210	
benzoic acid	0·75	18	high		—	—	1210	
copper	1	30	0·01		2·2	6·8	—	—
copper	4	340	0·02	0·07	0·7		—	—
copper	6	88	0·02		0·7		—	—
copper	9	88	0·02		0·7		—	—
copper	12	88	0·02		0·7		—	—
benzoic acid	0·5	—‖	high		—	—	819	1389
benzoic and adipic acids	0·38–0·75	—‖	high		—	—	1340	1525

† Nomenclature for definition of terms.
‡ Kinematic ratio defined as v_∞/v_i.
§ Sphere diameter expressed in inches.
‖ Data not used in evaluation of coefficients.

conditions of flow were of greater precision and accuracy than the local values. The local values of Nusselt number were constrained in the graphical analysis to satisfy the following integral expression involving the macroscopic data:

$$\int_0^{180^\circ} (Nu/Nu^*) \sin\psi \, d\psi = 2. \tag{5}$$

Transport rates at even values of the cosine of the polar angle were determined. The detailed local results together with the integral macroscopic values, as well as the average and standard deviations of the experimental data [13–15] from the smoothed curves, are available [29]. The sources of the experimental data are set forth in Table 1.

At levels of turbulence below 0·02, the following empirical relation [4] has been used in the past to approximate the behavior for local thermal transfer:

$$Nu = 2 + C(\psi)\, Re^m\, Pr_m^{\frac{1}{3}}. \tag{6}$$

The coefficient C and the exponent m are functions of polar angle, ψ. To illustrate the inadequacies of equation (6), the variation of the empirical exponent m with polar angle is shown in Fig. 2. The information obtained from equation (6) is primarily qualitative in nature since the value of the exponent is also a function of Reynolds number in the region near separation.

The effects of free-stream turbulence are of importance. The experimental data for spheres [13–15] indicate an effect similar to that obtained for cylinders by Giedt [6] and Seban [7]. Figure 3 depicts the local Frössling number for thermal and thermal with simultaneous material transfer as a function of the "apparent" level of longitudinal turbulence [30, 31] for several Reynolds numbers and polar angles for 0·5 and 1·0-in spheres [13–15]. The term "apparent" has been used to indicate that turbulence levels in the flowing air stream downstream of a grid were obtained from the detailed measurements of Davis [30, 31]. A similar configuration of the grid was used in the *onditions for data employed*†

Viscosity ratio‡		Range of data: Reynolds number		Range of data: Nusselt or Sherwood number		Source	Remarks
min.	max.	min.	max.	min.	max.		
1·36	1·38	800	7300	16	67	[15]	air jet
0·67	0·84	900	7300	18	41	[14]	air jet
0·835	0·837	1800	7500	24	64	[13]	air jet
1·0		50	1000	7	30	[1]	jet
—	—	490	7500	150	430	[5]	water tunnel
—	—	100	800	80	300	[4]	water tunnel
1·0	2·7	5	480000	0	1500	[16]	water tunnel
0·94		1800	200000	90	700	[8]	wind tunnel
—	—	87000	667000	300	800	[10]	wind tunnel
—	—	130000	1000000	314	1000	[10]	wind tunnel
—	—	177000	1200000	800	1500	[10]	wind tunnel
—	—	20	800	71	232	[2]	water tunnel
—	—	100	700	70	320	[3]	water tunnel

measurements on spheres [13–15] as employed by Davis. The experimental data for the 0·5 and 1·0 in spheres [13–15] are indistinguishable in the presentation of Fig. 3. The standard error of estimate in the Frössling number for the experimental data used to establish the full curves of Fig. 3 is indicated in the figure. The data [13–15] upon which Fig. 3 was based are shown as a function of the square root of the Reynolds number in Fig. 4. Within the uncertainty of measurement, the Frössling number is a linear function of the square root of the Reynolds number. The standard deviation of the experimental data from the curves of Fig. 4 is given in the lower part of Table 2 as a function of polar angle.

In the region of separated flow, which is encountered primarily in the aft hemisphere, the nature of the transport is different from that in the forward hemisphere. Figure 5 shows results in the aft hemisphere for thermal transport obtained from 0·5-in and 1·0-in silver spheres [13–14] and thermal with simultaneous material transport from a 0·5-in porous sphere [15]. No large effect from the level of turbulence was observed.

The data for local transport [13–15], together with those available from others [1, 4, 5, 8, 10, 16], are shown for thermal and for material transport with level of turbulence as a parameter in Figs. 6 and 7 for selected angles. The increases in Frössling number with increasing free-stream turbulence are strongest near stagnation and decrease continuously up to separation. The marked effect of polar angle upon the behavior is evident. The effects of transition begin to appear at a polar angle of about 70°. Instabilities in the flow appear as the Reynolds number is increased up to the critical value, above which the instabilities disappear. In the transition region, the characteristic instabilities become greater as the polar angle is increased. Much of the scatter of the experimental data may well result from the fluctuation in the position of the locus of separation. The absence of the effect of level of turbulence upon the local Frössling

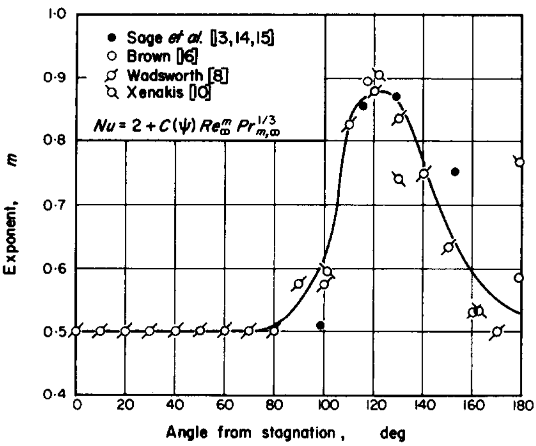

FIG. 2. Variation of exponent of equation (6) with polar angle.

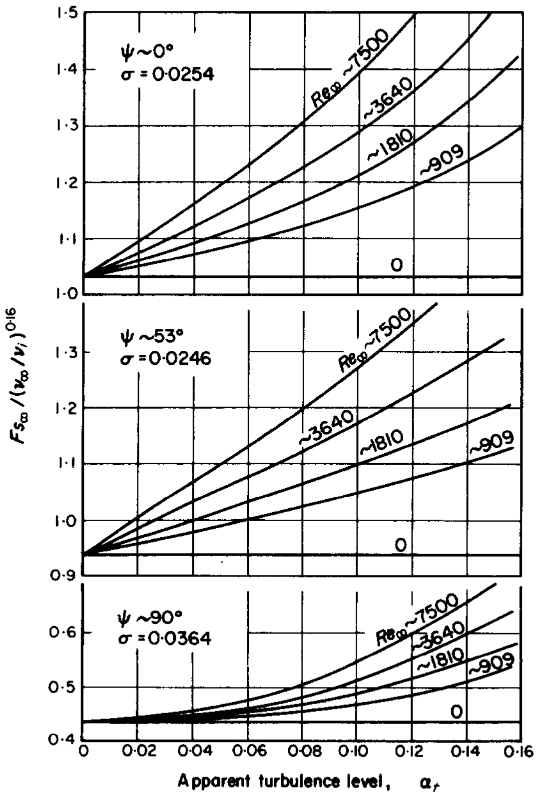

FIG. 3. Effect of level of turbulence upon local Frössling number.

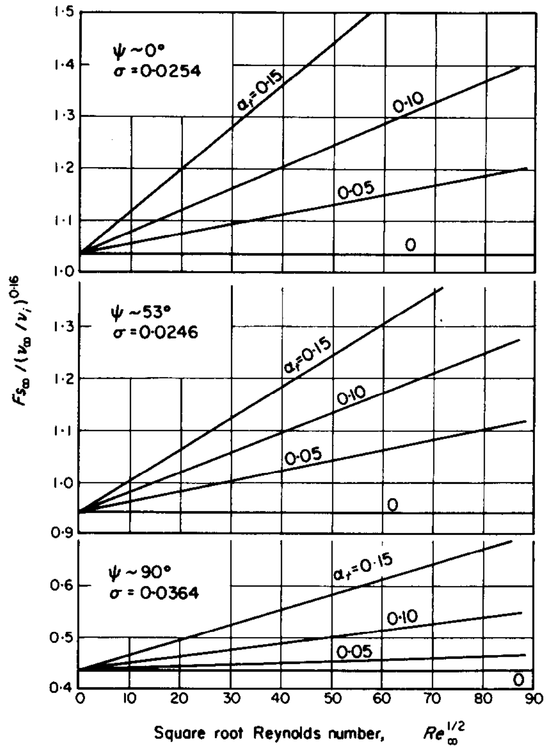

FIG. 4. Variation of local Frössling number with Reynolds number.

number is evident in Figs. 6 and 7 for the region aft of separation.

The effect of the scale of turbulence has not been investigated in detail. Maisel and Sherwood [32, 33] studied the effects of the intensity and of the scale of turbulence on the macroscopic thermal transport from spheres. The foregoing measurements indicated no effect of the scale of turbulence on the macroscopic thermal transport. The negative result may have been due to the fact that the integral scale of turbulence was only a fraction of the diameter of the spheres investigated. Van der Hegge Zijnen [34] carried out a similar experimental investigation involving cylinders and the scale of turbulence was varied over a wide range. These studies suggest that the effects of turbulence on the Frössling number are largest when the scale of

Table 2. Empirical coefficients for equations (7) and (8)†

Polar angle deg.	cos ψ	Number of data points used	rejected‡	Coefficient A	B	C	D	Deviation, fraction average§	standard‖
				Subcritical flow					
0	1·0	58	3	1·1849	0·2122	−0·1072	0·001317	0·00172	0·0453
36·9	0·8	59	2	1·1425	0·3001	−0·09403	0·001199	0·00209	0·0493
53·1	0·6	58	1	1·0143	0·3436	−0·09264	0·001466	0·00277	0·0556
66·4	0·4	63	1	0·8964	0·2859	−0·08356	0·0009623	0·000229	0·0498
78·5	0·2	59	2	0·7351	0·09017	—0·006822	0·0002934	0·00477	0·0748
90·0	0·0	54	5	0·5010	−0·03257	−0·4449	−0·0002787	0·0000618	0·0933
101·5	−0·2	55	3	0·2123	0·5087	−0·08828	0·001968	0·00214	0·180
113·6	−0·4	56	5	0·02280	0·3618	−0·09168	0·003743	0·0229	0·219
126·9	−0·6	61	4	0·1162	0·2351	−0·06142	0·003598	0·0344	0·182
143·1	−0·8	60	5	0·1882	0·1734	−0·07295	0·003797	0·0162	0·112
180·0	−1·0	61	2	0·2713	0·2333	−0·2001	0·005223	0·0570	0·243
				Supercritical flow					
0	1·0	42	1	1·4155	−0·09410	−0·9114	−0·00003900	0·000571	0·0243
36·9	0·8	44	0	1·3463	−0·01841	−0·1244	−0·00005591	0·000432	0·0206
53·1	0·6	26	0	1·3427	−0·006833	−0·4064	−0·0002765	0·000445	0·0216
66·4	0·4	38	0	1·0616	0·07020	−0·06481	0·0001322	0·000973	0·0318
78·5	0·2	42	1	0·9264	0·1043	−0·06476	0·00006054	0·000724	0·0294
90·0	0·0	29	1	0·4163	0·06141	−0·004980	0·0005782	0·00325	0·0633
101·5	−0·2	45	0	0·9220	0·4920	−0·08459	−0·00009771	0·0661	0·249
113·6	−0·4	38	2	0·8437	0·7592	−0·08504	0·0008995	0·0842	0·377
126·9	−0·6	39	0	1·3385	−0·2332	−0·1029	0·001379	0·0106	0·109
143·1	−0·8	39	0	1·1039	−0·2108	−0·02139	0·0005497	0·00480	0·0748
180·0	−1·0	31	0	0·09682	0·9612	−0·06214	0·003739	0·00374	0·0704
				Sage *et al.*, combined [13–15]					
0	1·0	28	2	1·0339	0·4447	−0·05925	0·003302	0·000592	0·0254
36·9	0·8	29	1	1·0041	0·2912	−0·04042	0·003246	0·000268	0·0243
53·1	0·6	28	2	0·9402	0·2284	−0·02158	0·002463	0·00139	0·0246
66·4	0·4	27	3	0·7726	0·2376	−0·03904	0·002429	0·00190	0·0256
78·5	0·2	26	4	0·6288	0·2964	−0·08141	0·001782	0·000119	0·0287
90·0	0·0	26	4	0·4372	0·2554	−0·08688	0·0009740	0·000312	0·0364
101·5	−0·2	27	3	0·1940	0·1618	−0·08770	0·001196	0·00287	0·0624
113·6	−0·4	30	0	0·08346	0·01362	0·09413	0·001591	0·00481	0·0806
126·9	−0·6	26	4	0·1711	0·06447	−0·02732	0·001687	0·0000293	0·0400
143·1	−0·8	24	6	0·2353	0·1543	−0·05513	0·001751	0·000865	0·0341
180·0	−1·0	26	4	0·2632	0·1691	−0·04860	0·001588	0·00151	0·0423

† Coefficients for equations

$$Fs_\infty = A(v_\infty/v_i)^{0.16} + [B\alpha_t(\alpha_t + C) + D]\, Re_\infty^{\frac{1}{2}}\, Pr_{m,\infty}^{\frac{1}{3}}$$

$$Fs_\infty = A(v_\infty/v_i)^{0.16} + [B\alpha_t(\alpha_t + C) + D]\, Re_\infty^{\frac{1}{2}}\, Sc_{m,\infty}^{\frac{1}{3}}.$$

‡ Statistically rejected when deviation exceeds 4σ.

§ Average deviation defined by

$$s = \frac{\sum_1^{N_p} \{w[(Fs_{\infty,e} - Fs_{\infty,c})/Fs_{\infty,e}]\}}{N_p}.$$

‖ Standard deviation defined by

$$\sigma = \left[\frac{\sum_1^{N_p} \{w[(Fs_{\infty,e} - Fs_{\infty,c})/Fs_{\infty,e}]^2\}}{N_p - N_c}\right]^{\frac{1}{2}}$$

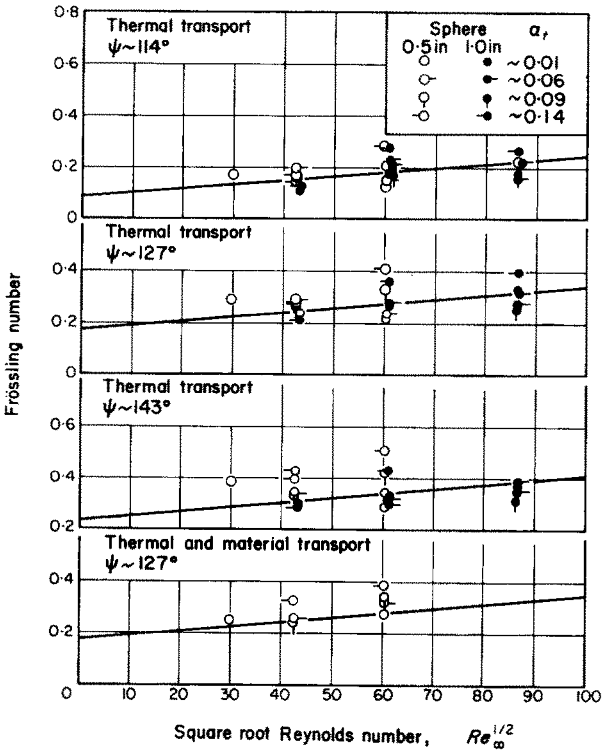

FIG. 5. Effect of Reynolds number in subcritical flow on local transport in aft hemisphere.

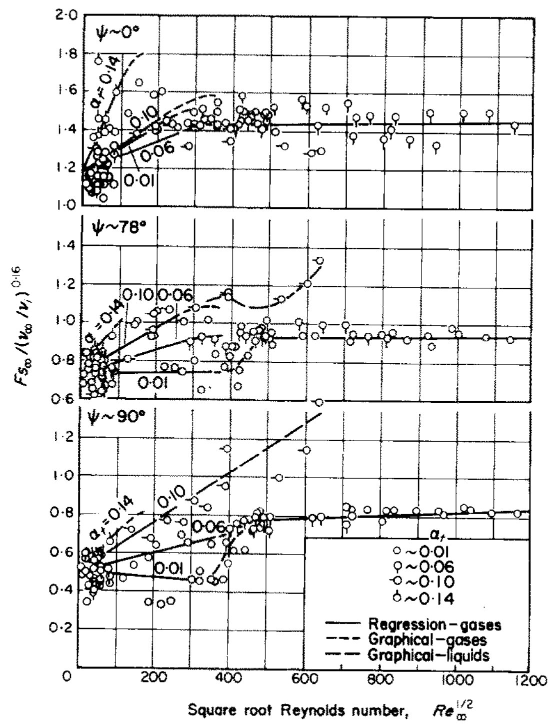

FIG. 6. Effect of Reynolds number on local transport in forward hemisphere.

turbulence is comparable to the diameter of the sphere.

There are several complicating factors in the analysis of data for either macroscopic [35] or local thermal or material-transport from spheres. Transport studies carried out with relatively large temperature or concentration differences involve significant variations of the molecular properties of the fluid in the boundary flows. The angular variation of the surface temperature and of the fugacity of the material in transport at the interface contribute to the difficulty of proper evaluation of the effect of variation of the molecular properties with position in the boundary flows. The variation in the specific weight of the fluid leads to natural convection in a gravitational field. Such effects become of importance in forced convection transport at a Reynolds number markedly less than 400. When material transport occurs at high rates, the effects of a momentum velocity normal to the surface alter the velocity profiles in such a way as to increase the thickness of the boundary flow.

Another significant difficulty in the interpretation of the experimental data is the "blockage" of a tunnel cross section by the sphere or other objects under investigation [36]. The maximum fraction of the cross section of the flow associated with the object involved in the data considered in this review was 0·16. The greater part of the data reported involved a blockage factor of approximately 0·07. Two effects result from such "blockage" [36, 37]. The average fluid velocity past the sphere is increased, and the wake is distorted as a result of wall constraints. A first-order correction employed in the current review involved the use of a Reynolds number, increased by the effect of area blockage on the average velocity.

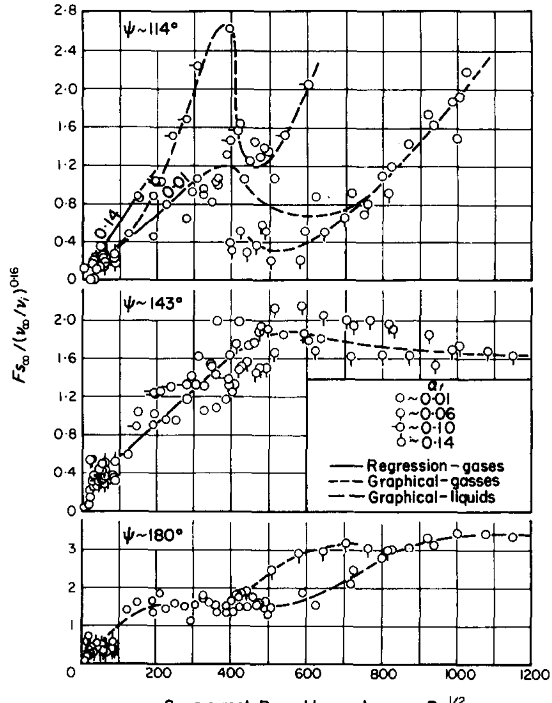

FIG. 7. Effect of Reynolds number on local transport in aft hemisphere.

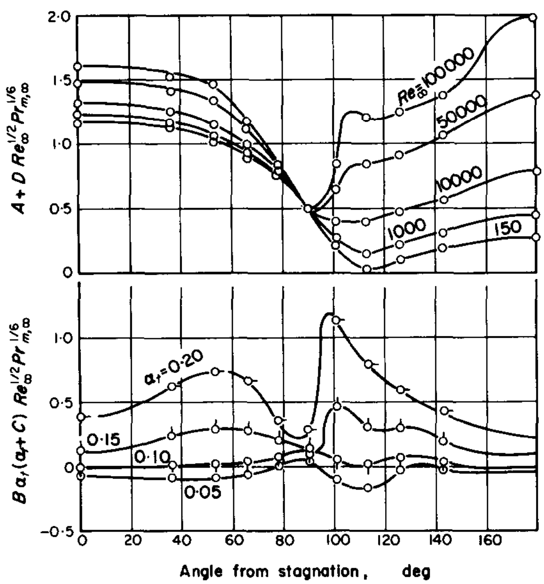

FIG. 8. Coefficients of equation (7) as a function of polar angle.

RESULTS

The objective of this discussion was the development of empirical relations which predict local thermal and material transport as a function of polar angle, Reynolds number, free-stream turbulence, molecular properties of the fluid in the free stream, and the variation of such properties through the boundary flow. The following expressions were obtained, in part, by theoretical considerations and, in part, by empirical statistical treatment of the experimental data. For subcritical flow, using data shown in Figs. 6 and 7 as a means of establishing the form of the relationships, the following empirical expression based upon the data listed in Table 1 resulted for thermal transport:

$$Fs_\infty = A\left(\frac{\nu_\infty}{\nu_i}\right)^{0.16} + [B\alpha_t(\alpha_t + C) + D] \times Re_\infty^{\frac{1}{2}}\, Pr_{m,\infty}^{\frac{1}{3}}. \qquad (7)$$

For material transport under the same type of conditions:

$$Fs_\infty = A\left(\frac{\nu_\infty}{\nu_i}\right)^{0.16} + [B\alpha_t(\alpha_t + C) + D] \times Re_\infty^{\frac{1}{2}}\, Sc_{m,\infty}^{\frac{1}{3}}. \qquad (8)$$

For supercritical flows the corresponding relations are:

$$Fs_\infty = A\left(\frac{\nu_\infty}{\nu_i}\right)^{0.16} + D\, Re_\infty^{\frac{1}{2}}\, Pr_{m,\infty}^{\frac{1}{3}}. \qquad (9)$$

$$Fs_\infty = A\left(\frac{\nu_\infty}{\nu_i}\right)^{0.16} + D\, Re_\infty^{\frac{1}{2}}\, Sc_{m,\infty}^{\frac{1}{3}}. \qquad (10)$$

The angular variation of the laminar and turbulent contributions for subcritical flow is shown in Fig. 8. The integral restraint of equation (5) was used to obtain agreement with the more accurate macroscopic measurements. In Table 2 the empirical coefficients have been tabulated for even values of the cosine of the polar angle together with a statistical measure of the agreement with the experimental data. It should be recognized that neither equations (7) and (8) nor equations (9) and (10) apply with accuracy in the region of transition between subcritical and supercritical boundary flows.

CONCLUSION

Analysis of available data reveals certain trends which appear to be in substantial agreement with the over-all transport theory. The effects of free-stream turbulent perturbations on the laminar layer are appreciable at the stagnation point and decrease up to the point of separation, while aft of separation only slight changes in transport are realized as a result of changes in free-stream turbulence. The effect of Reynolds number upon thermal transfer is greater aft of separation than in the forward hemisphere.

The transition and instabilities near separation were found to be influenced appreciably by free-stream turbulence. The increases in transport from increases in free-stream turbulence appear to attenuate as the laminar boundary flow develops into a turbulent boundary flow.

ACKNOWLEDGEMENTS

The senior author was the recipient of the Peter E. Fluor Memorial Fellowship and appreciation is expressed for the support thus afforded. Virginia Berry contributed to the regression analysis of the experimental data while Florence Nash aided in the preparation of the manuscript.

REFERENCES

1. N. Frössling, Über die Verdunstung Fallender Tropfen, *Beitr. Geophys.* **52** (1/2), 170 (1938).
2. F. H. Garner and R. W. Grafton, Mass transfer in fluid flow from a solid sphere, *Proc. R. Soc.* **A224**, 64 (1954).
3. F. H. Garner and R. D. Suckling, Mass transfer from a soluble solid sphere, *A.I.Ch.E. Jl* **4**, 114 (1958).
4. F. H. Garner and R. B. Keey, Mass transfer from single solid spheres—II, *Chem. Engng Sci.* **9**, 218 (1959).
5. M. Linton and K. L. Sutherland, Transfer from a sphere into a fluid in laminar flow, *Chem. Engng Sci.* **12**, 214 (1960).
6. W. H. Giedt, Effect of turbulence level of incident air stream on local heat transfer and skin friction on a cylinder, *J. Aeronaut. Sci.* **18**, 725 (1951).
7. R. A. Seban, The influence of free stream turbulence on the local heat transfer from cylinders, *J. Heat Transfer* **82**, 101 (1960).
8. J. Wadsworth, The experimental examination of the local heat transfer on the surface of a sphere when subjected to forced convective cooling, Nat. Res. Council Can., Div. Mech. Engng, Report No. MT-39 (1958).
9. L. G. Lautman and W. C. Droege, Thermal conductances about a sphere subjected to forced convection, Air Material Command, Serial No. AIRL A6118 50-15-3 (1950).
10. G. Xenakis, A. E. Amerman and R. W. Michelson, An investigation of the heat-transfer characteristics of spheres in forced convection, Wright Air Develop. Center, Wright–Patterson Air Force Base, Ohio, WADC Tech. Report 53-117 (1953).
11. A. E. Amerman, An investigation of the heat-transfer characteristics of spheres in forced convection, Wright Air Develop. Center, Wright–Patterson Air Force Base, Ohio, WADC Tech. Report 53-117, Suppl. 1 (1953).
12. J. R. Cary, The determination of local forced-convection coefficients for spheres, *Trans. Am. Soc. Mech. Engrs* **75**, 483 (1953).
13. E. Venezian, M. J. Crespo and B. H. Sage, Thermal and material transfer in turbulent gas streams: one-inch spheres, *A.I.Ch.E. Jl* **8**, 383 (1962).
14. W. W. Short, R. A. S. Brown and B. H. Sage, Thermal transfer in turbulent gas streams. Effect of turbulence on local transport from spheres, *J. Appl. Mech.* **27**, 393 (1960).
15. R. A. S. Brown and B. H. Sage, Material transfer in turbulent gas streams, *J. Chem. Engng Data* **6**, 355 (1961).
16. W. S. Brown, C. C. Pitts and G. Leppert, Forced convection heat transfer from a uniformly heated sphere, *J. Heat Transfer* **84**, 133 (1962).
17. I. Langmuir, The evaporation of small spheres, *Phys. Rev.* **12**, 368 (1918).
18. H. W. Morse, On evaporation from the surface of a solid sphere, *Proc. Am. Acad. Arts Sci.* **45**, 363 (1910).
19. N. Fuchs, Concerning the velocity of evaporation of small droplets in a gas atmosphere, *Phys. Z. Sowjun* **6**, 224 (1934); translated NACA, TM 1160.
20. N. Frössling, Evaporation, heat transfer, and velocity distribution in two-dimensional and rotationally symmetrical laminar boundary-layer flow, NACA TM 1432, Washington, D.C. (1958).
21. I. Korobkin, Discussion of local laminar heat transfer coefficients for spheres and cylinders in incompressible flow, Am. Soc. Mech. Engrs Preprint 54-F-18 Rev. (1955).
22. A. C. Lochiel and P. H. Calderbank, Mass transfer in the continuous phase around axisymmetric bodies of revolution, *Chem. Engng Sci.* **19**, 471 (1964).
23. E. Ruckenstein, On mass transfer in the continuous phase from spherical bubbles or drops, *Chem. Engng Sci.* **19**, 131 (1964).
24. L. B. Torobin and W. H. Gauvin, Fundamental aspects of solids-gas flow, *Can. J. Chem. Engng* **37**, 167 (1959).
25. K. Lee and H. Barrow, Some observations on transport processes in the wake of a sphere in low speed flow, *Int. J. Heat Mass Transfer* **8**, 403 (1965).
26. P. D. Richardson, Estimation of the heat transfer from the rear of an immersed body to the region of separated flow, AD-290339, ARL 62-423 (1962).
27. P. D. Richardson, Heat and mass transfer in turbulent separate flows, *Chem. Engng Sci.* **18**, 149 (1963).

28. A. R. BÜYÜKTÜR, J. KESTIN and P. F. MAEDER, Influence of combined pressure gradient and turbulence on the transfer of heat from a plate, *Int. J. Heat Mass Transfer* **7**, 1175 (1964).
29. T. R. GALLOWAY and B. H. SAGE, Document A 9765, Am. Doc. Inst., Washington 25, D.C. (196). $1.25 for photoprints or $1.25 for 35 mm microfilm.
30. L. DAVIS, Measurements of turbulence decay and turbulent spectra behind grids, Jet Propulsion Laboratory, Calif. Inst. Tech., Pasadena, Calif., Report No. 3–17 (June 1952).
31. L. DAVIS, Measurements of turbulence level behind a set of square-mesh grids and correlations with grid pressure loss, Jet Propulsion Laboratory, Calif. Inst. Tech., Pasadena, Calif., Report No. 3–22 (November 1950).
32. D. S. MAISEL and T. K. SHERWOOD, Evaporation of liquids into turbulent gas streams, *Chem. Engng Prog.* **46**, 131 (1950).
33. D. S. MAISEL and T. K. SHERWOOD, Effect of air turbulence on rate of evaporation of water, *Chem. Engng Prog.* **46**. 172 (1950).
34. B. G. VAN DER HEGGE ZIJNEN, Heat transfer from horizontal cylinders to a turbulent air flow, *Appl. Sci. Res.* **7A**, 205 (1957–1958).
35. T. R. GALLOWAY and B. H. SAGE, Thermal and material transport from spheres. Prediction of macroscopic thermal and material transport, *Int. J. Heat Mass Transfer* **10**, 1195 (1967).
36. E. C. MASKELL, A theory of the blockage effects on bluff bodies and stalled wings in a closed wind tunnel, Royal Aircraft Estab., Rept. No. Aero 2685 (November 1963).
37. G. C. VLIET and G. LEPPERT, Forced convection heat transfer from an isothermal sphere to water, *J. Heat Transfer* **83**, 163 (1961).

Résumé—On a établi des expressions, à partir d'un examen des données expérimentales disponibles sur le transport thermique et de matière local, à partir de sphères, afin de permettre la prédiction de ce transport en fonction du nombre de Reynolds, de l'intensité de la turbulence et de l'angle polaire. On a trouvé que l'effet du nombre de Reynolds était plus prononcé dans l'écoulement décollé sur l'hémisphère aval que dans les couches limites de l'hémisphère amont. En outre, l'intensité de la turbulence exerçait un effet beaucoup plus prononcé sur le transport local dans l'hémisphère amont que dans l'hémisphère aval. Les résultats sont présentés en fonction du nombre de Frössling.

Zusammenfassung—Auf Grund der verfügbaren Versuchsdaten über den lokalen Wärme- und Stofftransport von Kugeln wurden Beziehungen abgleitet, die die Berechnung des Transports als Funktion der Reynolds-Zahl, der Turbulenzintensität und des Polwinkels erlauben. Es ergab sich, dass der Einfluss der Reynolds-Zahl in der abgelösten Strömung der hinteren Halbkugel ausgeprägter war, als in der Grenzschichtströmung der vorderen Halbkugel. Andererseits hatte die Turbulenzintensität einen viel ausgeprägteren Einfluss auf den lokalen Transport in der vorderen Halbkugel als in der hinteren. Die Ergebnisse werden in Abhängigkeit von der Frössling-Zahl angegeben.

Аннотация—На основе известных из литературы экспериментальных данных о локальном тепло-и массопереносе от сфер выведены зависимости переноса от числа Рейнольдса, интенсивности турбулентности и полярного угла. Влияние числа Рейнольдса оказывается более существенным для отрывного течения на задней полусфере, нежели для пристенных течений на передней части сферы. С другой стороны, интенсивность турбулентности гораздо больше влияла на локальный перенос в передней полусфере. Результаты обобщены с помощью числа Фрёсслинга.